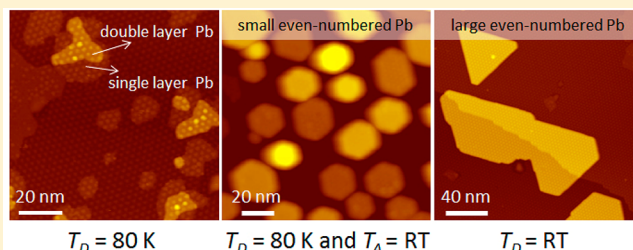


# Growth and Structural Properties of Pb Islands on Epitaxial Graphene on Ru(0001)

L. W. Liu, W. D. Xiao, K. Yang, L. Z. Zhang, Y. H. Jiang, X. M. Fei, S. X. Du, and H.-J. Gao\*

Institute of Physics, Chinese Academy of Sciences, P.O. Box 603, Beijing 100190, China

**ABSTRACT:** Structural properties of Pb islands grown on graphene/Ru(0001) at various deposition temperatures ( $T_D$ ) and annealing temperatures ( $T_A$ ) are investigated by a low-temperature scanning tunneling microscope. Single-layer Pb islands with a  $2 \times 2$  reconstruction are only formed at  $T_D$  of 80 K and disappear with post-annealing to room temperature (RT). It is revealed that a morphological transition of the Pb islands takes place, from irregular shapes to a hexagonal equilibrium shape, with increasing  $T_D$  or  $T_A$  to RT. Moreover, Pb islands grown at  $T_D$  of RT are larger than those grown at a  $T_D$  of 80 K and annealed to RT. All Pb islands with a  $T_A$  or  $T_D$  of RT are (111)-faceted with thicknesses of even-numbered atomic layers and exhibit a weak interaction between Pb and graphene.



## INTRODUCTION

Graphene, a single sheet of carbon atoms arranged in a honeycomb lattice, is an ideal two-dimensional (2D) material that has attracted great interest because of its unique electronic structure, high carrier mobility, and relativistic quantum phenomena.<sup>1–3</sup> In recent years, the epitaxial growth and electronic structures of graphene on SiC and a variety of transition metal substrates have been studied intensively.<sup>4–12</sup> Meanwhile, the structural and physical/chemical properties of foreign materials grown on graphene<sup>13–15</sup> are also important issues for both fundamental research and potential applications. Dispersive and size-uniform transition metal nanoclusters for potential applications in catalysis and magnetic data storage have been fabricated on graphene using graphene moiré patterns as templates.<sup>16–18</sup> Recently, extended Pb islands have been grown on graphene/SiC (G/SiC), and a weak interaction between Pb islands and graphene substrate has been proposed.<sup>19</sup> However, despite the great importance of the morphology and size of Pb islands to the electronic properties<sup>20–27</sup> (e.g., quantum size effects and superconductivity), a systematic study of the growth and structural evolution of Pb islands grown on graphene moiré templates is still needed.

In this work, we study the structural and initial growing properties of Pb islands on graphene/Ru(0001) (G/Ru) resulting from different deposition substrate temperatures ( $T_D$ ) and annealing temperatures ( $T_A$ ) by a low-temperature scanning tunneling microscope (LT-STM). Single-layer and irregular-shaped bilayer Pb islands have been successfully constructed at a  $T_D$  of 80 K. We observe a morphological transition of the Pb islands from irregular shapes to hexagons after post-annealing to room temperature (RT), and Pb islands grow larger as  $T_D$  increases, approaching RT. All Pb islands with  $T_A$  or  $T_D$  of RT are (111)-faceted with thickness of even

atomic layers. These even-layered Pb islands are quasi-free-standing because of a weak interfacial Pb–C coupling.

## EXPERIMENTAL AND CALCULATION DETAILS

The experiments were conducted with an ultrahigh-vacuum (UHV) LT-STM system (Unisoku) at a base pressure of  $1 \times 10^{-10}$  mbar. The Ru(0001) surface was prepared by repeated cycles of sputtering with argon ions and annealing to 950 °C. High quality, large-area monolayer graphene was obtained via pyrolysis of ethylene on Ru(0001) substrate that was held at 950 °C.<sup>8</sup> The Pb source was made from a piece of Pb (purity of 99.999%) wrapped by a tungsten wire that can be heated up via passing current. The Pb source was thoroughly degassed prior to Pb deposition. The typical deposition rate was  $\sim 0.01$  monolayer (ML)/min ( $1 \text{ ML} = 9.4 \times 10^{14} \text{ atoms/cm}^2$ , corresponding to a single layer of bulk Pb(111)), as calibrated by STM. The G/Ru(0001) substrate was held at either 80 K (by liquid nitrogen cooling) or RT during Pb deposition. All STM images were acquired at 77 K in constant-current mode with electrochemically etched tungsten tips, and the given voltages refer to the sample.

Density functional theory (DFT) calculations were carried out using the Vienna ab initio simulation package (VASP) with the local-density approximation (LDA). The periodic slab model contains  $2 \times 2$  graphene and one Pb atom. In this model, all atoms were fully relaxed until the net force on each atom was less than 0.01 eV/Å. In our calculations the k-sampling was  $21 \times 21 \times 1$ , and the energy cutoff of the plane-wave basis sets was 400 eV.

Received: April 28, 2013

Revised: October 5, 2013

Published: October 8, 2013



## RESULTS AND DISCUSSION

Monolayer graphene prepared on Ru(0001) substrate exhibits a regular moiré pattern with a periodicity of  $\sim 3$  nm due to the lattice mismatch between graphene and the Ru(0001) surface.<sup>8</sup> After Pb deposition of  $\sim 0.6$  ML at  $T_D$  of 80 K, we transfer the sample immediately to the STM at 77 K and observe the formation of two-dimensional (2D) islands of Pb on G/Ru, as shown in Figure 1a. A hexagonal superstructure stemming from

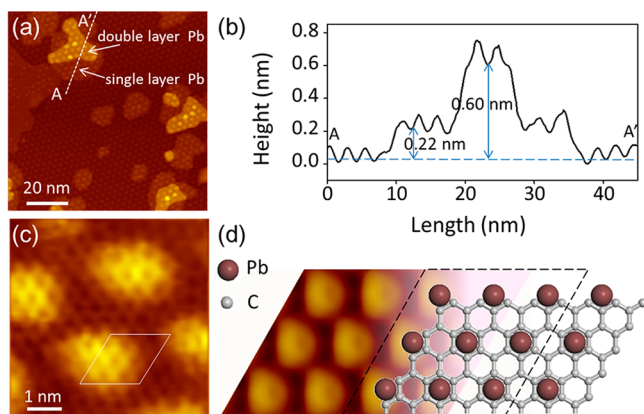


**Figure 1.** Pb islands with  $T_D$  of 80 K. (a) STM image of single-layer and bilayer Pb islands (96 nm  $\times$  96 nm,  $U = -2.5$  V,  $I = 3.4$  pA). (b) Line profile of the dotted line in (a). (c) Zoom-in image of single-layer Pb island showing the atomic distance of 500 pm (5.5 nm  $\times$  5.5 nm,  $U = -1$  V,  $I = 0.4$  pA). (d) Simulated STM image (left panel) with the model of  $(2 \times 2)$  Pb–C reconstruction (right panel), which reproduces the main feature in the white rhombus of (c).

the moiré pattern of graphene is observable as a modulation of these Pb islands, revealing that these extended 2D Pb islands cross several unit cells of the graphene moiré pattern. A line profile analysis (Figure 1b) reveals that the Pb islands have apparent heights of either 0.22 or 0.60 nm with respect to G/Ru. Considering that a single atomic step of bulk Pb(111) has a height of 0.28 nm, we assign these islands to be single-layer or bilayer Pb islands, respectively. Single-layer Pb islands show a hexagonal structure with a lattice constant of 0.5 nm (Figure 1c), twice that of graphene. Thus, the single-layer Pb islands are actually  $2 \times 2$  superstructures with respect to the graphene lattice. To figure out the adsorption site of Pb atoms with respect to the graphene layer, we performed DFT calculations. The  $2 \times 2$  Pb superstructure on G/Ru(0001) is modeled by a  $2 \times 2$  Pb superstructure on a free-standing graphene layer, each unit cell including one Pb atom and eight carbon atoms. Three possible adsorption sites (hollow, bridge, and atop) of Pb atoms with respect to the free-standing graphene layer are considered. Our calculations show that the hollow site, where a Pb atom is placed at the hexagonal center of underlying carbon atoms, is the most stable adsorption site. The binding energy is about 60 meV lower than that of the top site and 41 meV lower than that of the bridge site. Figure 1d illustrates the STM simulation (left panel) with the structural model (right panel) of single-layer Pb island on G/Ru(0001), where each yellow protrusion in the STM simulation corresponds to the one Pb atom. The STM simulation reproduces the main feature of the atomic-resolution STM image (see the white rhombus in Figure 1c) and confirms the  $2 \times 2$  Pb superstructure, although the ripple of the moiré pattern is not considered in our simulation.

While the single-layer Pb islands have a lattice constant of 0.5 nm, the bilayer Pb islands show a hexagonal lattice with an atomic periodicity of 0.33 nm, slightly smaller than the lattice constant of 0.35 nm for Pb(111) surface. As a hexagonal shape is expected for the (111)-faceted Pb island at its thermodynamic equilibrium state, the frequently observed irregular shaped Pb islands grown on G/Ru (Figure 1a) indicate that the  $T_D$  of 80 K is not high enough for the bilayer Pb islands to reach their thermodynamic equilibrium shapes. From an atomic diffusion point of view,<sup>28–30</sup> the edge diffusion and kink crossing processes have already been activated at 80 K, leading to the formation of compact (111)-faceted Pb islands, whereas the kink and corner breaking processes requiring higher activation energies<sup>28</sup> are probably hindered, resulting in nonequilibrium shapes of these Pb islands.

The formation of extended 2D Pb islands across several unit cells of the graphene moiré pattern at the low temperature of 80 K is very similar to that of Pb grown on G/SiC<sup>19</sup> and HOPG.<sup>31</sup> This 2D growth is different from the formation of dispersive metal nanoclusters at the specific sites of graphene moiré patterns, such as Pt clusters on G/Ru.<sup>17</sup> The growth of dispersive metal nanoclusters is due to the inhomogeneous electronic structures of the graphene moiré patterns and relatively strong interaction between Pt atoms and graphene. This indicates that the interaction between Pb and G/Ru is comparatively weak, and the growth is mainly dominated by the cohesive interaction between Pb atoms. It is also noteworthy that the formation of single-layer Pb islands with  $2 \times 2$  superstructures like those observed in our current study is absent in previous reports of Pb growth on G/SiC and graphite.<sup>19,32</sup>

The single-layer Pb islands disappear and the bilayer Pb islands take a hexagonal shape after post-annealing to RT for 10 min, as seen in Figure 2a. The disappearance of single layer Pb islands indicates that such  $2 \times 2$  superstructures are not stable at RT and that the Pb–Pb interaction is dominant over the

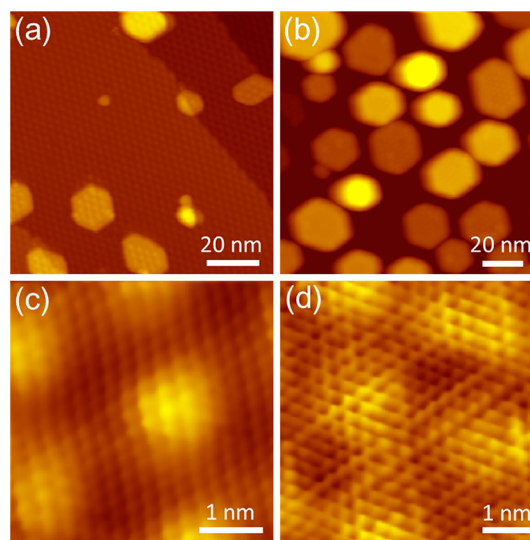


**Figure 2.** Pb islands with  $T_D$  of 80 K and annealed to RT. (a) Pb islands at low coverage, showing hexagonally shaped islands (100 nm  $\times$  100 nm,  $U = -2$  V,  $I = 47$  pA). (b) Pb islands at high coverage, with small lateral size of less than 30 nm (127 nm  $\times$  127 nm,  $U = -4.3$  V,  $I = 8.3$  pA). (c) Atomic resolution STM image of bilayer Pb island (5 nm  $\times$  5 nm,  $U = -0.2$  V,  $I = 74$  pA). (d) Atomic resolution STM image of 4-layer Pb island (7 nm  $\times$  7 nm,  $U = -4$  mV,  $I = 50$  pA).



Pb–C interaction. The transition of the bilayer Pb islands from the irregularly shaped morphology to the hexagonal equilibrium shape after post-annealing demonstrates that the kink and corner breaking processes have been activated at RT.<sup>28</sup> After repeated cycles of Pb deposition at  $T_D$  of 80 K and post-annealing to RT, a large number of Pb islands with an average lateral size of  $\sim 20$  nm are formed on G/Ru at a total Pb coverage of  $\sim 3$  ML, as shown in Figure 2b. Line profile analysis discloses island heights of 0.6, 1.2, and 1.8 nm with respect to G/Ru(0001), corresponding to the island thickness of 2, 4, and 6 layers of Pb, respectively. High-resolution STM images of bilayer and four-layer Pb islands reveal hexagonal lattices with average atomic distances of 0.33 and 0.36 nm, respectively (Figure 2c,d). These values are close to the lattice constant ( $\sim 0.35$  nm) of bulk Pb(111).

For comparison, we also studied the growth of Pb on G/Ru at RT, as shown in Figure 3a with  $\sim 0.16$  ML Pb coverage.

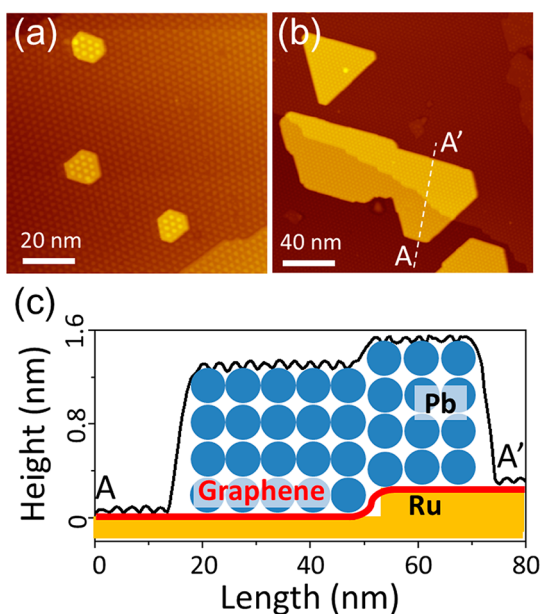


**Figure 3.** Pb islands with  $T_D$  of RT. (a) Pb islands at low coverage, showing hexagonal shape ( $100\text{ nm} \times 100\text{ nm}$ ,  $U = -2.7\text{ V}$ ,  $I = 4.2\text{ pA}$ ). (b) Pb islands at higher coverage, showing a large island merged from two islands ( $200\text{ nm} \times 200\text{ nm}$ ,  $U = -2\text{ V}$ ,  $I = 5\text{ pA}$ ). (c) Line profile of the dotted line in (b); a schematic of the carpet growth model is added.

Unlike the observation at  $T_D$  of 80 K, no single-layer Pb island is observed at the  $T_D$  of RT, evidencing that the weak interaction between Pb and graphene at higher  $T_D$  does not favor the wetting of single layer Pb on G/Ru. Besides, all Pb islands show the equilibrium shape of hexagons, similar to Pb islands grown at 80 K with subsequent post-annealing to RT. With increasing Pb coverage, the Pb islands grow in lateral sizes and thickness. At Pb coverage of  $\sim 1$  ML, large Pb islands with lateral sizes over 100 nm can be found (Figure 3b). As identified from the contour of the large Pb island, it results from merging of two Pb islands with hexagonal shape, which is different from the formation of small and densely packed Pb islands at  $T_D$  of 80 K and subsequent annealing to RT (Figure 2b). This demonstrates that the diffusion at RT is more efficient, which helps to grow large islands. The different growth behaviors can be understood according to the nucleation theory of epitaxy.<sup>30</sup> The nucleation density is

inversely proportional to the diffusion coefficient, which is exponentially related to the deposition temperature. Therefore, high deposition temperature results in low nucleation density and therefore favors the formation of large Pb islands, which is the case of Pb deposited on G/Ru at RT.

Interestingly, the growth of Pb islands is not impeded by the steps of G/Ru(0001). Instead, the Pb islands can grow across the steps of G/Ru(0001) and extend over several terraces, as shown in Figure 3b. The line profile analysis (Figure 3c) reveals that different parts of the island, whether on the upper or on the lower terraces of step edges, have the same thickness, and the whole island has the equilibrium shape, as if the steps were absent. This carpet-like growth mode of Pb on G/Ru is very similar to that of graphene grown on Ru(0001), where the graphene sheet grows continuously across the steps of Ru(0001) and covers the steps like a carpet. A schematic model of this carpet-like growth mode of Pb on G/Ru(0001) is shown under the line profile in Figure 3c.

It is notable that Dil and co-workers observed a formation of only even-numbered Pb films for Pb grown on epitaxial graphite at 100 K by means of photoemission spectroscopy, and their first-principles calculations revealed a magic stability of even-numbered free-standing Pb films, which suggest a weak interfacial Pb–C coupling.<sup>32</sup> Thus, our similar observation that all Pb islands with the  $T_A$  or  $T_D$  of RT have thicknesses of evenly numbered layers suggests that the Pb islands on G/Ru are quasi-free-standing. When imaging Pb islands on graphene continuously, the drag-up of a large part of a Pb island by the STM tip can be observed (see Figure 4a,b), further confirming the weak interaction between Pb and graphene.

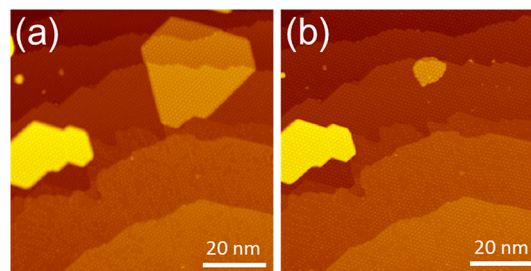


**Figure 4.** Weak interaction between Pb and graphene. (a, b) Consecutive STM images showing the drag-up of a large part of a Pb island ( $85\text{ nm} \times 85\text{ nm}$ ,  $V = 2.5\text{ V}$ ,  $I = 0.1\text{ nA}$ ), demonstrating a weak interaction between Pb and graphene.

The absence of odd-numbered Pb islands on graphene or graphite surfaces is different from that of Pb growth on Si(111), where odd-numbered Pb films still can be observed despite their stability being weaker than that of the even-numbered ones.<sup>24</sup> The reason for such different behaviors for Pb growth on G/Ru and Si(111) relies on the different electronic structures at the interfaces between Pb and substrates. In contrast to the relatively weak interfacial coupling between Pb and G/Ru, the active dangling bonds of the Si(111) surfaces result in very strong Pb–Si bonding and the formation of a stable wetting layer of Pb on Si(111). The different interfacial coupling and structures of Pb on G/Ru and Pb on Si(111) lead to different surface energies and stabilities of odd- and even-numbered Pb islands/films.

## SUMMARY

We investigate the growth and structural properties of Pb islands on G/Ru employing a LT-STM. The formation of extended 2D Pb islands on G/Ru at  $T_D$  of 80 K and RT is observed. Single-layer Pb islands with a  $2 \times 2$  reconstruction are constructed only at a  $T_D$  of 80 K. It is revealed that the morphology of the Pb islands transforms from irregular shapes to hexagonal equilibrium shape with increasing  $T_D$  or  $T_A$  of RT. All Pb islands except the single-layer ones are (111)-faceted with thicknesses of an even number of atomic layers. These even-numbered Pb islands are quasi-free-standing because of a weak interfacial Pb–C coupling. Our results provide useful information about the interfacial structures and properties of Pb on graphene, which will be helpful for tuning the superconductivity and quantum size effects of Pb islands grown on graphene.

## AUTHOR INFORMATION

### Corresponding Author

\*E-mail: hjgao@iphy.ac.cn (H.-J.G.).

### Notes

The authors declare no competing financial interest.

## ACKNOWLEDGMENTS

Financial support from the NSFC (51210003, 11290165), National “973” project (2009CB929103 and 2010CB923004) of China, and the CAS is gratefully acknowledged.

## REFERENCES

- (1) Novoselov, K. S.; Geim, A. K.; Morozov, S. V.; Jiang, D.; Zhang, Y.; Dubonos, S. V.; Grigorieva, I. V.; Firsov, A. A. Electric field effect in atomically thin carbon films. *Science* **2004**, *306*, 666–669.
- (2) Zhang, Y. B.; Tan, Y. W.; Stormer, H. L.; Kim, P. Experimental observation of the quantum Hall effect and Berry's phase in graphene. *Nature* **2005**, *438*, 201–204.
- (3) Castro Neto, A. H.; Guinea, F.; Peres, N. M. R.; Novoselov, K. S.; Geim, A. K. The electronic properties of graphene. *Rev. Mod. Phys.* **2009**, *81*, 109–162.
- (4) Zhou, S. Y.; Gweon, G. H.; Fedorov, A. V.; First, P. N.; De Heer, W. A.; Lee, D. H.; Guinea, F.; Neto, A. H. C.; Lanzara, A. Substrate-induced bandgap opening in epitaxial graphene. *Nat. Mater.* **2007**, *6*, 770–775.
- (5) Rutter, G. M.; Crain, J. N.; Guisinger, N. P.; Li, T.; First, P. N.; Stroscio, J. A. Scattering and interference in epitaxial graphene. *Science* **2007**, *317*, 219–222.
- (6) Pan, Y.; Shi, D. X.; Gao, H. J. Formation of graphene on Ru(0001) surface. *Chin. Phys. Lett.* **2007**, *16*, 3151–3153.
- (7) Sutter, P. W.; Flege, J. I.; Sutter, E. A. Epitaxial graphene on ruthenium. *Nat. Mater.* **2008**, *7*, 406–411.
- (8) Pan, Y.; Zhang, H. G.; Shi, D. X.; Sun, J. T.; Du, S. X.; Liu, F.; Gao, H. J. Highly ordered, millimeter-scale, continuous, single-crystalline graphene monolayer formed on Ru (0001). *Adv. Mater. (Weinheim, Ger.)* **2009**, *21*, 2777–2780.
- (9) Winterlin, J.; Bocquet, M. L. Graphene on metal surfaces. *Surf. Sci.* **2009**, *603*, 1841–1852.
- (10) Coraux, J.; N'Diaye, A. T.; Busse, C.; Michely, T. Structural coherency of graphene on Ir(111). *Nano Lett.* **2008**, *8*, 565–570.
- (11) Li, X. S.; Cai, W. W.; An, J. H.; Kim, S.; Nah, J.; Yang, D. X.; Piner, R.; Velamakanni, A.; Jung, I.; Tutuc, E.; Banerjee, S. K.; Colombo, L.; Ruoff, R. S. Large-area synthesis of high-quality and uniform graphene films on copper foils. *Science* **2009**, *324*, 1312–1314.
- (12) Gao, M.; Pan, Y.; Zhang, C. D.; Hu, H.; Yang, R.; Lu, H. L.; Cai, J. M.; Du, S. X.; Liu, F.; Gao, H. J. Tunable interfacial properties of epitaxial graphene on metal substrates. *Appl. Phys. Lett.* **2010**, *96*, 053109.
- (13) Zhou, S. Y.; Siegel, D. A.; Fedorov, A. V.; Lanzara, A. Metal to insulator transition in epitaxial graphene induced by molecular doping. *Phys. Rev. Lett.* **2008**, *101*, 086402.
- (14) Zhou, H. T.; Mao, J. H.; Li, G.; Wang, Y. L.; Feng, X. L.; Du, S. X.; Mullen, K.; Gao, H. J. Direct imaging of intrinsic molecular orbitals using two-dimensional, epitaxially-grown, nanostructured graphene for study of single molecule and interactions. *Appl. Phys. Lett.* **2011**, *99*, 153101.
- (15) Zhang, H. G.; Sun, J. T.; Low, T.; Zhang, L. Z.; Pan, Y.; Liu, Q.; Mao, J. H.; Zhou, H. T.; Guo, H. M.; Du, S. X.; Guinea, F.; Gao, H. J. Assembly of iron phthalocyanine and pentacene molecules on a graphene monolayer grown on Ru(0001). *Phys. Rev. B* **2011**, *84*, 245436.
- (16) N'Diaye, A. T.; Bleikamp, S.; Feibelman, P. J.; Michely, T. Two-dimensional Ir cluster lattice on a graphene moiré on Ir(111). *Phys. Rev. Lett.* **2008**, *97*, 215501.
- (17) Pan, Y.; Gao, M.; Huang, L.; Liu, F.; Gao, H. J. Directed self-assembly of monodispersed platinum nanoclusters on graphene Moiré template. *Appl. Phys. Lett.* **2009**, *95*, 093106.
- (18) Sicot, M.; Bouvron, S.; Zander, O.; Rudiger, U.; Dedkov, Y. S.; Fonin, M. Nucleation and growth of nickel nanoclusters on graphene moiré on Rh(111). *Appl. Phys. Lett.* **2010**, *96*, 093115.
- (19) Hupalo, M.; Liu, X. J.; Wang, C. Z.; Lu, W. C.; Yao, Y. X.; Ho, K. M.; Tringides, M. C. Metal nanostructure formation on graphene: Weak versus strong bonding. *Adv. Mater. (Weinheim, Ger.)* **2011**, *23*, 2082–2087.
- (20) Guo, Y.; Zhang, Y. F.; Bao, X. Y.; Han, T. Z.; Tang, Z.; Zhang, L. X.; Zhu, W. G.; Wang, E. G.; Niu, Q.; Qiu, Z. Q.; Jia, J. F.; Zhao, Z. X.; Xue, Q. K. Superconductivity modulated by quantum size effects. *Science* **2004**, *306*, 1915–1917.
- (21) Qin, S. Y.; Kim, J.; Niu, Q.; Shih, C. K. Superconductivity at the two-dimensional limit. *Science* **2009**, *324*, 1314.
- (22) Eom, D.; Qin, S.; Chou, M. Y.; Shih, C. K. Persistent superconductivity in ultrathin Pb films: A scanning tunneling spectroscopy study. *Phys. Rev. Lett.* **2006**, *96*, 027005.
- (23) Zhang, T.; Cheng, P.; Li, W. J.; Sun, Y. J.; Wang, G.; Zhu, X. G.; He, K.; Wang, L. L.; Ma, X. C.; Chen, X.; Wang, Y. Y.; Liu, Y.; Lin, H. Q.; Jia, J. F.; Xue, Q. K. Superconductivity in one-atomic-layer metal films grown on Si(111). *Nat. Phys.* **2010**, *6*, 104–108.
- (24) Ma, X. C.; Jiang, P.; Qi, Y.; Jia, J. F.; Yang, Y.; Duan, W. H.; Li, W. X.; Bao, X.; Zhang, S. B.; Xue, Q. K. Experimental observation of quantum oscillation of surface chemical reactivities. *Proc. Natl. Acad. Sci. U. S. A.* **2007**, *104*, 9204–9208.
- (25) Brun, C.; Hong, I. P.; Patthey, F.; Sklyadneva, I. Y.; Heid, R.; Echenique, P. M.; Bohnen, K. P.; Chulkov, E. V.; Schneider, W. D. Reduction of the superconducting gap of ultrathin Pb islands grown on Si(111). *Phys. Rev. Lett.* **2009**, *102*, 207002.
- (26) Wang, K. D.; Zhang, X. Q.; Loy, M. M. T.; Chiang, T. C.; Xiao, X. D. Pseudogap mediated by quantum-size effects in lead islands. *Phys. Rev. Lett.* **2009**, *102*, 076801.
- (27) Nishio, T.; An, T.; Nomura, A.; Miyachi, K.; Eguchi, T.; Sakata, H.; Lin, S. Z.; Hayashi, N.; Nakai, N.; Machida, M.; Hasegawa, Y. Superconducting Pb island nanostructures studied by scanning tunneling microscopy and spectroscopy. *Phys. Rev. Lett.* **2008**, *101*, 167001.
- (28) Bogicevic, A.; Stromquist, J.; Lundqvist, B. I. Low-symmetry diffusion barriers in homoepitaxial growth of Al(111). *Phys. Rev. Lett.* **1998**, *81*, 637–640.
- (29) Zhang, Z. Y.; Lagally, M. G. Atomistic processes in the early stages of thin-film growth. *Science* **1997**, *276*, 377–383.
- (30) Brune, H. Microscopic view of epitaxial metal growth: nucleation and aggregation. *Surf. Sci. Rep.* **1998**, *31*, 121–229.
- (31) Brun, C.; Müller, K. H.; Hong, I. P.; Patthey, F.; Flindt, C.; Schneider, W.-D. Dynamical coulomb blockade observed in nanosized electrical contacts. *Phys. Rev. Lett.* **2012**, *108*, 126802.
- (32) Dil, J. H.; Kampen, T. U.; Hulsén, B.; Seyller, T.; Horn, K. Quantum size effects in quasi-free-standing Pb layers. *Phys. Rev. B* **2007**, *75*, 161401.